Supplemental Figures

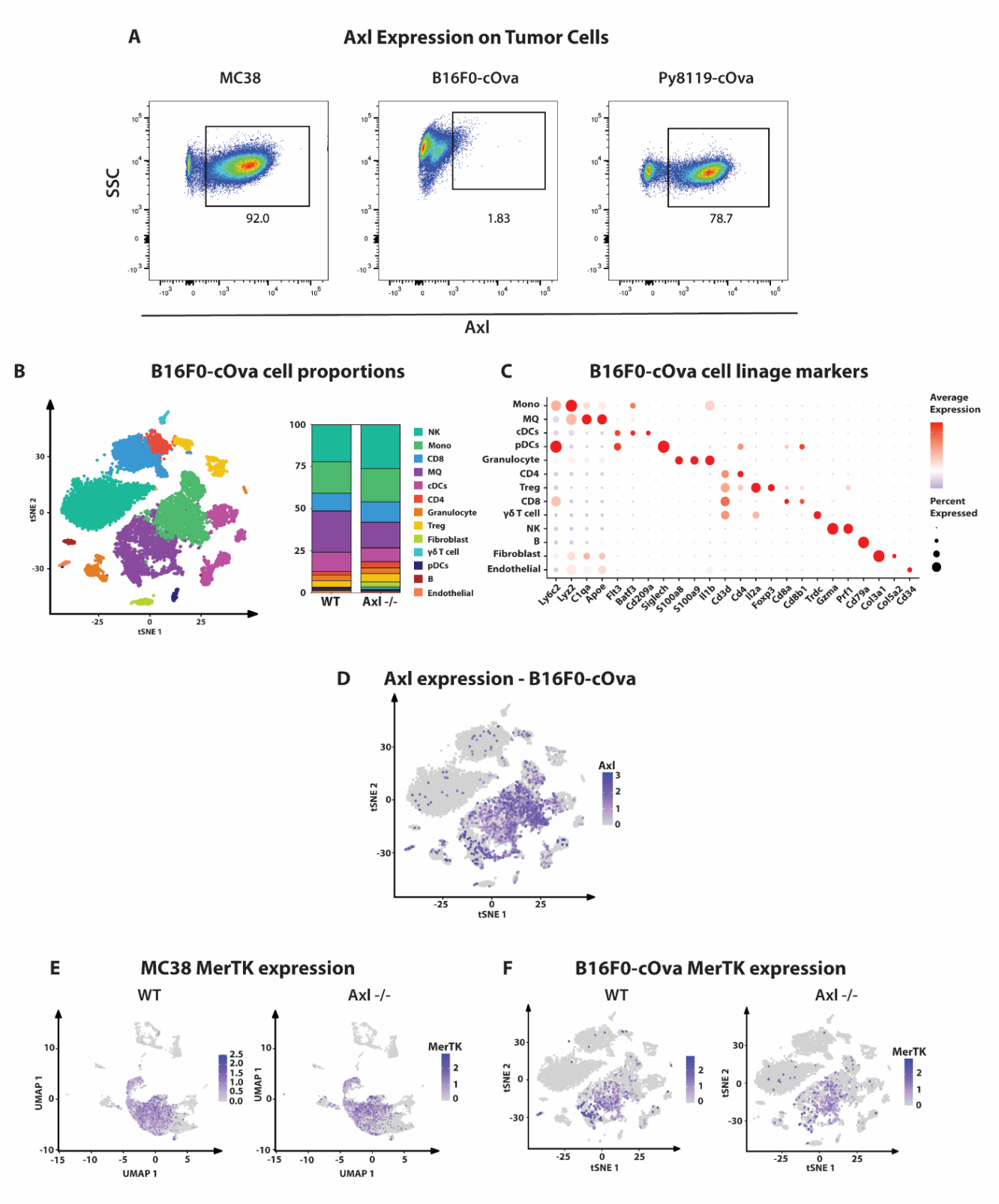

Supplemental Figure 1.

(**A**) Flow cytometry plots displaying levels of Axl expression on MC38, B16F0-cOva and Py8119-cOva cell lines. (**B)** TSNE projection illustrating the intratumoral immune cell populations in B16F0-cOva tumors merged between Wild type and $Axl^{-/-}$ host (left panel) and the proportions between each genotype (right panel). (**C**) Heatmap displaying canonical cell type markers used to annotate immune cell clusters. (**D)** TSNE projection illustrating expression levels of Axl across individual immune cell clusters. (**E-F)** UMAP and TSNE projections showing MerTK expression levels in both WT and Axl KO mice across MC38 and B16F0-cOva tumor models respectively.

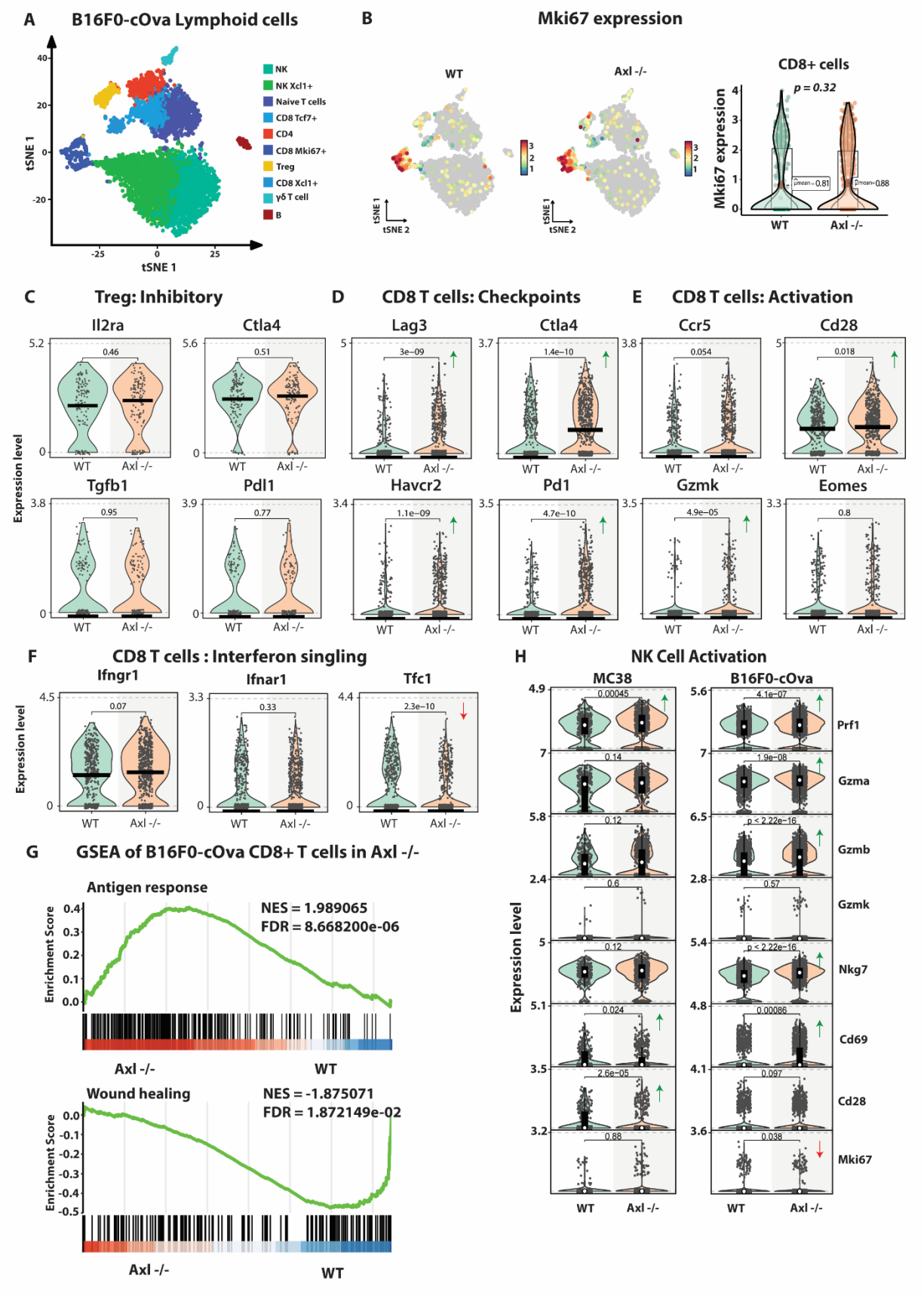

Supplemental Figure 2.

(**A**) UMAP projection subset on lymphoid cells in B16F0-cOva tumor-bearing mice merged between WT and Axl KO (n= 6302 cells). **(B)** UMAP projection illustrating KI67 expression on intratumoral lymphoid cells in B16F0-cOva tumors (left panel). Violin plot comparing Ki67 expression levels between $CD8^+$ T cells found in WT and Axl KO mice (right panel). (**C-F),** Violin plots comparing gene expression levels of inhibitory molecules on Treg cells **(C),** immune checkpoints on $CD8^+$ T cells **(D),** activation markers on $CD8^+$ T cells (**E**), and interferon signaling associated molecules between WT and Axl KO mice (**F**). (**G**) Gene set enrichment analysis reveals enhanced antigen response pathways and reduced wound healing pathways in $CD8^+$ T cells from Axl KO mice compared to WT. (**H**) Violin plots comparing expression levels of activation markers on NK cells from WT and Axl KO mice in both MC38 and B16F0-cOva tumors.

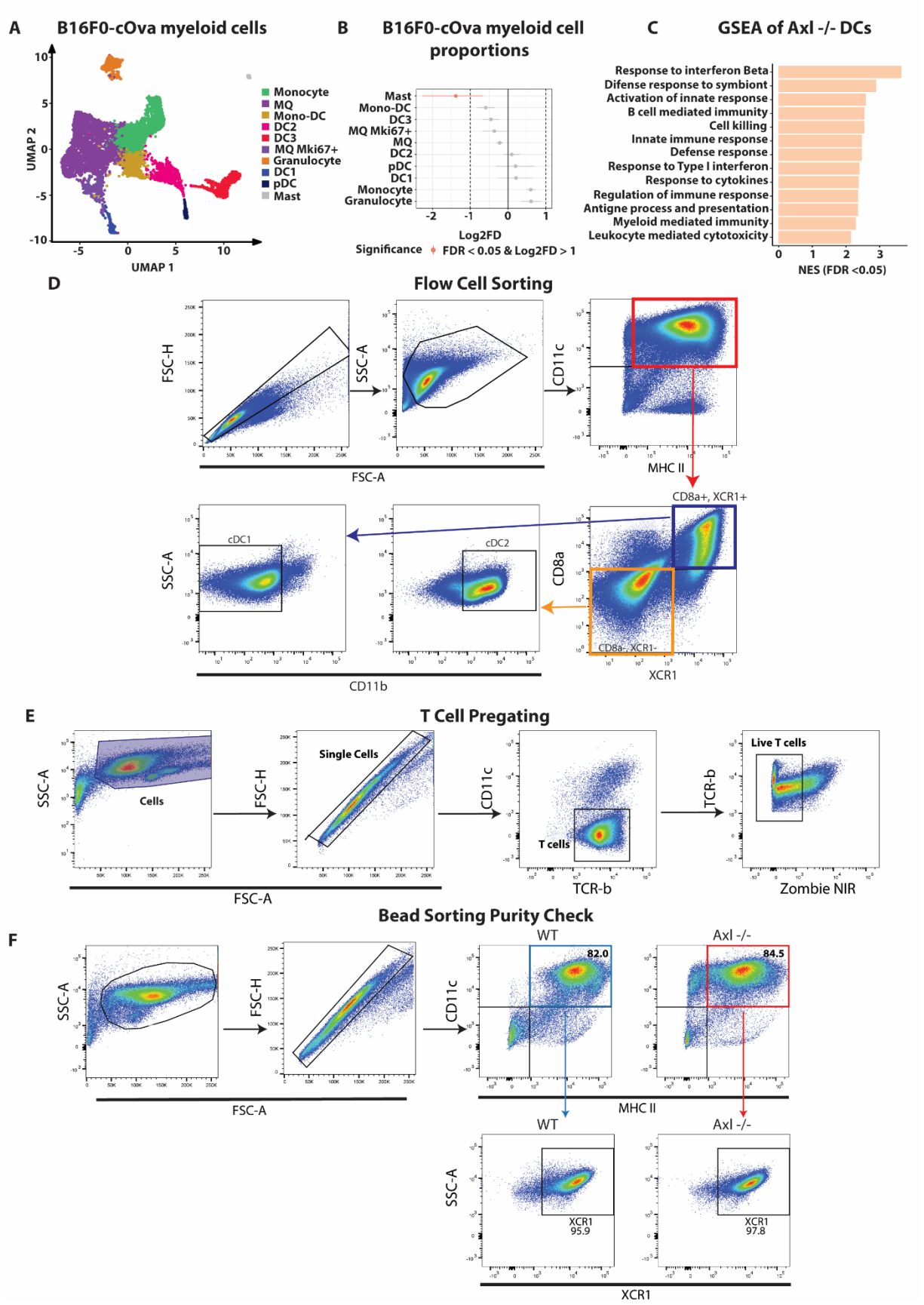

Supplemental Figure 3

(A) UMAP projection merged between WT and Axl KO mice subset on myeloid cells in B16F0-cOva tumors (n=7441 cells). (**B)** Plot illustrating distribution of cellular population between WT and Axl KO mice. **(C)** GSEA depicting top signaling pathways enriched in DCs from Axl KO mice over WT. **(D)** Flow cytometry plots depicting the flow sorting strategy for splenic DC1 and DC2 cells. **(E)** Flow cytometry plots illustrating OTI CD8+ T cell pre-gating strategy. (**F**) Flow cytometry plots depicting cell purity post DC1 bead sorting.

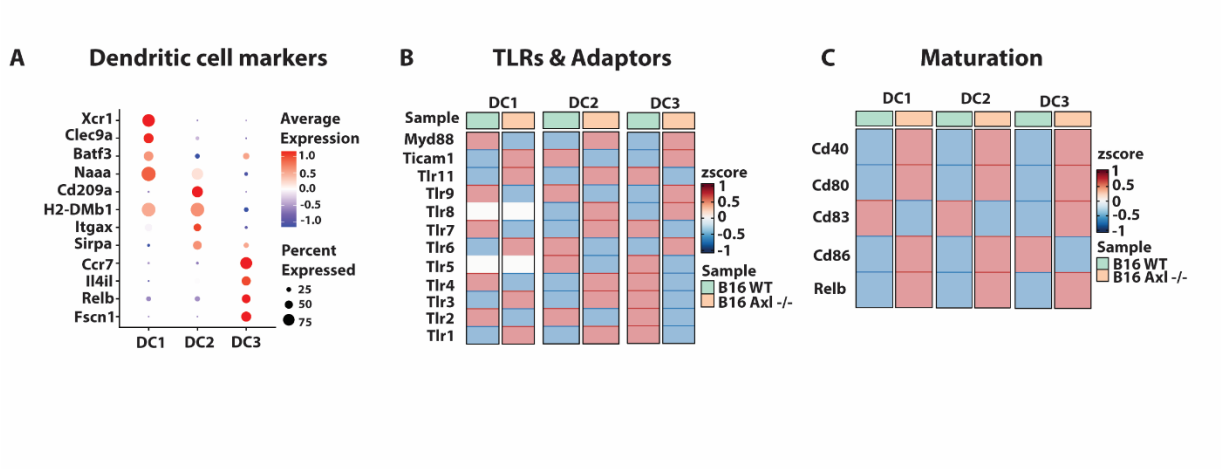

Supplemental Figure 5

(**A**) Flow plot displaying immunophenotyping markers for DC1, DC2, and DC3 subpopulations found in B16F0-cOva tumors. (**B**) Heatmap comparing expression scores of toll like receptors and adapter proteins between WT and Axl -/- DC subpopulations. (**C**) Heatmap comparing expression of maturation markers between WT and Axl -/- DC subpopulations.